IMAV2017-44
https://www.imavs.org/pdf/imav.2017.44

Propeller Performance Calculation for Multicopter Aircraft at Forward Flight Conditions and Validation with Wind Tunnel Measurements

C. Molter*, P.W. Cheng,
University of Stuttgart, Wind Energy Research Group (SWE) at the Institute of Aircraft Design
Allmandring 5b, 70569 Stuttgart, Germany

ABSTRACT

When designing a fast flying multicopter aircraft knowledge about propellers at inclined inflow conditions is important. To investigate this operating condition a whirl tower was built and several propellers were tested in a wind tunnel at angles of attack of $8°$, $15°$, $22.5°$ and $30°$. The inflow speeds were varied between $4\ m/s$ and $30\ m/s$.
The gained measurement data was used to validate an in-house blade element simulation software. The simulations were improved by adjusting airfoil lift and drag polars to static propeller measurements. Without any further adjustments to the inclined inflow condition the simulations showed good agreement with the measurements of two different propellers operating at an angle of attack. This means that it is possible for future projects to gain significant knowledge about propellers at an angle of attack with the use of static thrust and performance measurements without the need for a wind tunnel.
A less complicated semi-analytical approach was also tested to model the performance of propellers at an angle of attack. Without further adjustments to the equations it was not possible to achieve a good agreement with measurement data using the simplified approach.
Some measurements were also taken with a counter-rotating propeller arrangement (coaxial rotors). A hypothesis is proposed that the thrust deficit of the bottom propeller due to the influence of the top propeller is less at forward flight conditions than at the static operating condition. This hypothesis could be confirmed by measurements but still needs further validation.

1 INTRODUCTION

In the scope of the ANWIND project a multicopter aircraft for wind measurements near wind turbines will be designed, built and tested at the University of Stuttgart's Wind Energy Research Group (SWE). The two main challenges in the development process of this aircraft, called ANDroMeDA (ANWIND Drone for Measurement and Data Acquisition) are a reasonable performance in terms of stable flight at windy conditions and long flight duration as well as placing the measurement probe away from disturbances of the propellers.
Since ANDroMeDA will be hovering at wind speeds of $11\ m/s$ ((the design wind speed of a wind turbine) and above it is important to have knowledge on how the propellers will perform at an angle of attack and at higher inflow speeds. Without experiences on thrust and power of inclined propellers it is even impossible to make a statement about the resulting flight times.
For static propeller operation or propellers with a straight inflow (airplane operation) several open source simulation tools exist e.g. Qprop, JavaProp, JBlade [1, 2, 3] and some measurement data is also available [4]. Hence it is more or less easy to calculate the hover performance of a multicopter rotor in the absence of wind.
For a multicopter that is designed to be able to hover in strong headwinds or a multicopter designed to be most efficient at higher forward flight speeds the available simulation tools cannot be used and propeller measurements are really rare. Larger helicopter companies have their own in-house blade element simulation tools. There are also commercial tools available for example CAMRAD [5]. Since those commercial tools are above the budget of most UAV projects and are capable of much more than needed for this task the UAV department at the SWE developed a small custom made blade element tool, called *RotoCalc*, which is able to simulate inclined propellers.
Since *RotoCalc* could not be validated with measurement data in the past and since no wind tunnel measurements for inclined propellers are available for the desired propeller sizes a propeller test rig, called whirl tower, was built and several propellers have been tested at inclined inflow conditions. Two propellers, an APC Thin Electric 13x6.5 and an Aeronaut CAM Carbon Light 13x6 have been simulated. Because a counter-rotating propeller configuration is also considered for the ANDroMeDA multicopter to achieve a higher redundancy another test rig was built for this propeller arrangement additionally.

*Email address: molter@ifb.uni-stuttgart.de

IMAV2017-44
https://www.imavs.org/pdf/imav.2017.44

2 Description of the Test Setup and Simulation Environment

2.1 Whirl Tower Setup

The whirl tower is shown in Figure 1 and Figure 2. It measures propeller thrust, propeller torque, propeller RPM, battery voltage, motor current,motor temperature and the current ESC input signal. All measurements are transmitted to a PC at a rate of 50 Hz. Thrust and torque measurements are taken using low cost load cells [6] and low cost load cell amplifiers [7]. To make sure no aerodynamic forces will disturb the load cells the whirl tower is covered with a clear plastic cylinder. The RPM is determined electronically with the help of one phase of the brushless motor.
All electronics is placed on a single circuit board included in the whirl tower to keep cable lengths short. The whirl tower is connected to the data acquisition laptop via bluetooth. This ensures a galvanic isolation. The PC software (Figure 3) displays all measurements in real time. It is also possible to send commands e.g. for taring the load cells and to control the motor power with this software.
To calibrate the torque and force measurements a special arrangement of pulleys and wires has been designed shown in Figure 2. The friction of the pulleys at loaded condition could be determined to be less than 3 g. During calibration the maximum relative error in thrust was about 0.6% and the maximum relative error in torque was about 1.6%. For most load conditions these errors were much smaller.
The RPM measurement quality is hard to characterize since it is not known if deviations are originated in the measurement or in the ESC and motor. After comparison with a strobe lamp the measurement accuracy is assumed to be about ± 10 RPM. Another source for measurement errors is the whirl tower itself and its aerodynamic wake which is of course larger than in the usual multicopter arrangement with a thin motor arm.

2.2 Counter-Rotating Propeller Test Setup

For the counter-rotating propellers another test setup was used. The thrust of the upper and lower propeller is measured separately with the same kind of load cells used for the whirl tower [6]. The RPM of the upper and lower propeller as well as the motor current of upper and lower motor is also measured separately. Additionally the battery voltage is measured. Figure 4 shows the test setup.
Unfortunately the mounting stiffness of the connection between load cells and motors was too low so that oscillations occurred. These oscillations only occurred with the wind tunnel running. All static tests were not influenced by oscillations. Since the wind tunnel time was limited and the problem was not revealed before the campaign there was no time to improve the motor mounts. The load cell stiffness itself is much higher than the stiffness of the motor mounts so that thicker motor mounts, also resulting in a slightly higher propeller distance, should eliminate this problem for future measurements. The distance of the two propeller is 70 mm from blade tip to blade tip in the current setup.

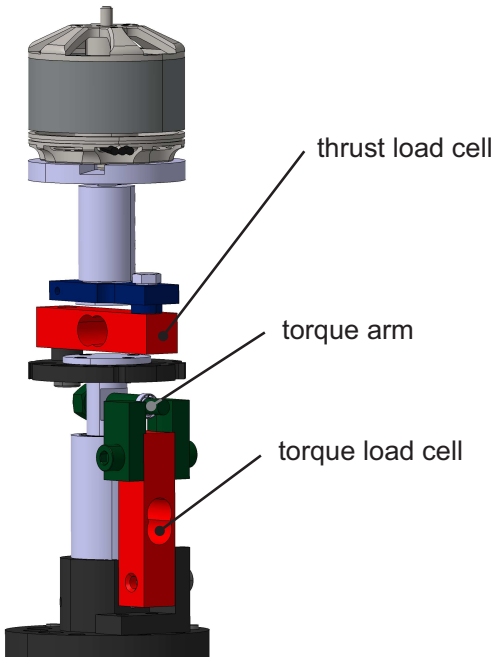

Figure 1: Load cell arrangement at the whirl tower.

2.3 Wind-Tunnel Setup

The experiments described in this article were conducted in the medium size low speed wind tunnel at the Institute Aerodynamics and Gas Dynamics (IAG) at the University of Stuttgart. This wind tunnel is a closed Gttinger type tunnel with an open jet test section. The nozzle used has a diameter of 1.0 m. Since the whirl tower and counter-rotating propeller test rig are working completely independent from all other equipment no further measurements were needed from

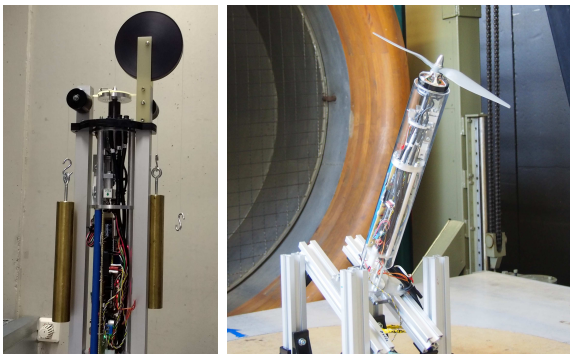

Figure 2: Left: Calibration Unit with a pair of torque calibration weights applied; Right: Whirl tower mounted in the wind tunnel and tilted forward.

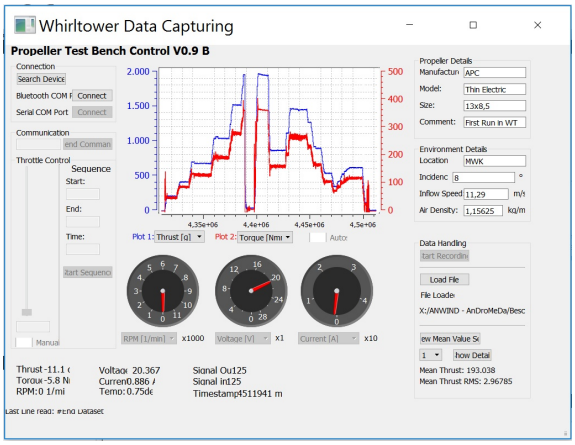

Figure 3: Software to control the whirl tower and save measurements.

the wind tunnel except the wind speed measurement. The wind speed measurement is accomplished with a pitot tube, a static pressure hole and very accurate humidity and temperature sensors. Since the whirl tower measurements were averaged over time during post processing and since the wind tunnel speed fluctuates only very little the time averaged wind speed was transferred from hand to the whirl tower control software and saved with each measurement file.

2.4 *Simulation Software RotoCalc and Simulation Settings*

The Software *RotoCalc* uses the blade element method as described for example in [8] and [9]. Since this procedure is a pretty standard approach a more detailed description is not part of this article and only the relevant settings are described. The induced velocity can be determined in three different ways with *RotoCalc*. Two of them were used for this investigation. For the static case the well-known Blade Element Combined Momentum Method (also called BEMT) was used. This method determines an induced velocity in a way that each annular ring of the rotor disc will produce the same thrust whether calculated by simple momentum theory or by two dimensional airfoil theory. More information can be found for example in [8] or [9]. The method will result in a non-uniform induced velocity along the blade radius.
RotoCalc is also able to use the BEMT method for an inclined propeller. But it appeared that this results in a less accurate agreement with wind tunnel measurements. For the inclined propeller operation a uniform velocity along the rotor disc resulted in a better agreement with measurement data. The induced velocity v_i at the propeller disc for a propeller inclined by the angle α_{prop} and operated at the thrust T while experiencing an inflow speed V_∞ is determined by:

$$v_i = \frac{T}{2\rho A_{prop} V_{res}} \quad (1)$$

$$V_{res} = \sqrt{(sin(\alpha_{prop})V_\infty + v_i)^2 + (cos(\alpha_{prop})V_\infty)^2} \quad (2)$$

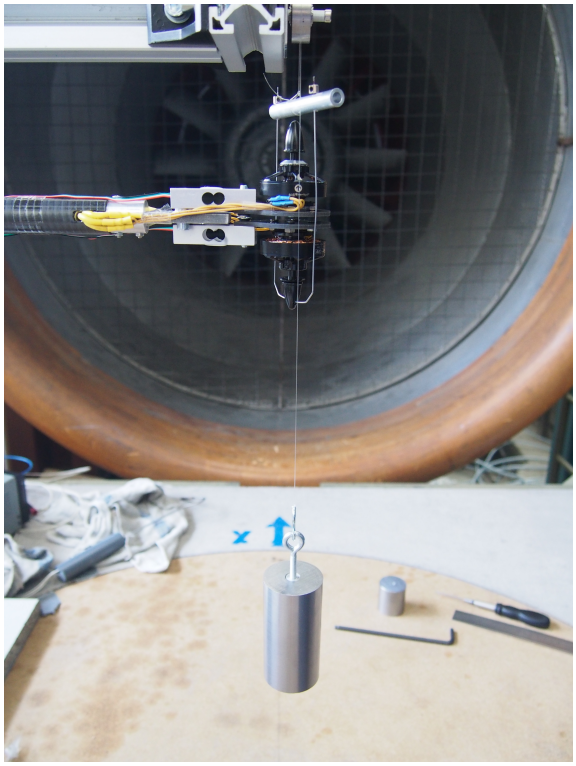

Figure 4: Counter-rotating propeller test setup with calibration weight for the bottom load cell applied.

Where A_{prop} is the propeller disc area and ρ is the air density. This semi-empirical equation was first formulated by Glauert [10]. The equation cannot be solved analytically. *RotoCalc* solves this equation numerically after each full revolution using the false position method. This is done till the thrust evaluated by Equation 1 and the the thrust evaluated by two-dimensional airfoil theory / blade element theory converge.
Tip-losses are modeled quite simple with Prandtl's tip-loss factor as described for example in [9]. Therefore the blade element thrust is neglected at the thrust integration after a certain radial position. This radial position is called the effective blade radius R_e. It is decreased by the factor B. $B = 0.95$ was used for this simulations.
The propeller blades can be modeled in *RotoCalc* by several radial positions. For each position blade chord and twist as well as the airfoil to use can be set. Between those radial positons *RotoCalc* will interpolate linearly. The number of blade elements to use for the interpolation can be set to an arbitrary number. For the APC propeller an overall number of 96 radial elements was used and for the Aeronaut Propeller an overall number of 99 radial elements was used. A finer resolution did not show any change of the simulations results.
Since the inclined propeller does not experience a rotational symmetric inflow it also has to be discretized in the azimuth

IMAV2017-44
https://www.imavs.org/pdf/imav.2017.44

direction. The azimuth step size can be set freely with *RotoCalc*. For both simulations 72 azimuth steps ($\Delta\Psi = 5°$) have been used. A finer resolution did not change the results.
In-plane or out-of-plane bending as well as twisting of the propeller was not considered. The propeller was modeled as a totally rigid propeller without flapping or lagging. In *RotoCalc* different airfoils and hence different lift and drag polars can be set up. If two different airfoils are set for two following radial positions both airfoils will be taken into account and *RotoCalc* will interpolate between the two resulting lift and drag coefficients of both airfoils.
The airfoils are specified by look up tables with an arbitrary number of angles of attack. To account for Reynolds number effects several lift and drag polars can be set at several Reynolds numbers for each airfoil .
Instead of a look up table an equations can also be used to model lift and drag. This was used to adjust the polars to a better agreement with static measurements as described below. The angle of attack for a propeller can be set between $\alpha_{prop} = 0°$ (helicopter rotor in hover or climb / airplane propeller) and $\alpha_{prop} = 90°$ (helicopter rotor with parallel inflow).

3 Static Propeller Measurements

As preparation for the wind tunnel measurements a number of 18 two-bladed propellers and two three-bladed propellers between 13 inch and 14 inch diameter have been tested at static operation on the whirl tower. A complete list of the results will not be given here. On one hand it is beyond the scope of this article to give an extensive propeller market overview. On the other hand it is really hard to tell which propeller is the best regarding the maximum thrust at a given power or the highest figure of merit for a given thrust. It can be said that the aerodynamic performance of most of the propellers was not differing very much and differences were often located in the range of measurement uncertainties. Because the propellers are very similar regarding the aerodynamic performance other factors like price and weight start to play a more important role.
Two general remarks can be given: Wooden propellers had a slightly lower figure of merit than those made of plastics. This can be explained by their higher relative airfoil thickness resulting from the lower structural strength of the material. Expensive carbon fiber propellers could not proof to have a better aerodynamic performance. At least not in the range of the accuracy given by the whirl tower. But these propellers have of course a lower weight which will result in a higher weight remaining for the flight battery and hence in an increased overall flight performance.

4 Propeller Modeling

Two different propellers were modeled for BE simulations: An APC Thin Electric 13x6 and an Aeronaut CAM Carbon Light 13x6 propeller. The geometric properties were determined purely manual using a caliper, angle templates and cutting the propeller at several blade positions to estimate the used airfoils / proper airfoils to estimate the propeller performance. A more sophisticated method, e.g. involving a 3D scanner, could be used in the future of course to decrease the remaining geometric uncertainties.
After determining airfoils with suitable thickness and camber lift and drag polars between $\alpha = -30°$ and $\alpha = +30°$ have been determined at several Reynolds numbers with the help of the two-dimensional panel method simulation software XFOIL [11]. To be able to adapt the simulations to measurements by fine-tuning the polars, the XFOIL results were then described by the following analytical equations:

$$c_l(\alpha) = cl0 + cla \cdot \alpha \tag{3}$$

$$c_d(c_l) = cd0 + cd2(c_l - clcd0)^2 \tag{4}$$

$$cd2 = cd2u \;\; if \;\; c_l < clcd0 \tag{5}$$

$$cd2 = cd2l \;\; if \;\; c_l < clcd0 \tag{6}$$

By using these coefficients it is possible to adjust a polar towards higher/lower lift and higher/lower drag without editing every single line in the polar lookup table. Modeling lift- and drag-polars with these coefficients can also be found in QProp [1] and therefore additionally results in the possibility to compare static *RotoCalc* simulations to QProp simulations easily.

5 Fine-Tuning of Simulations

Figure 5 and figure 6 show the measurement results for the APC and Aeronaut propeller in comparison with the initial and the tuned simulations. The initial simulations have been done without any further adjustments to measurement data. Propeller chord and twist were modeled according to geometric measurements and the initial lift and drag polars from XFOIL [11] runs have been used.
Those initial simulations not only suffer from uncertainties which airfoil is really used for the actual propeller but also the flow at a rotating propeller can be quite complex. It includes three-dimensional effects like the effect of centrifugal force on the blade's boundary layer, low Reynolds number effects as well as additional turbulence introduced to the boundary layer by the rotating propeller. Some observations and a comparison between BE simulations, three-dimensional CFD simulations and an experiment can be found in [12]. Because of this circumstances without measurement data the initial simulations can only be seen as a first guess. To the author's knowledge it is also quite common for the development of manned helicopters to adjust BE simulations to whirl tower measurements by fine-tuning lift and drag polars.
By manually adjusting the lift and drag polars at three different Reynolds numbers, corresponding propeller operation at $n = 2000\ RPM$, $n = 4500\ RPM$ and $n = 7000\ RPM$, a very good match between simulation and measurement could be achieved for the static propeller operation. It has to be em-

phasized that all this steps can be done completely without the necessity of wind tunnel measurements.

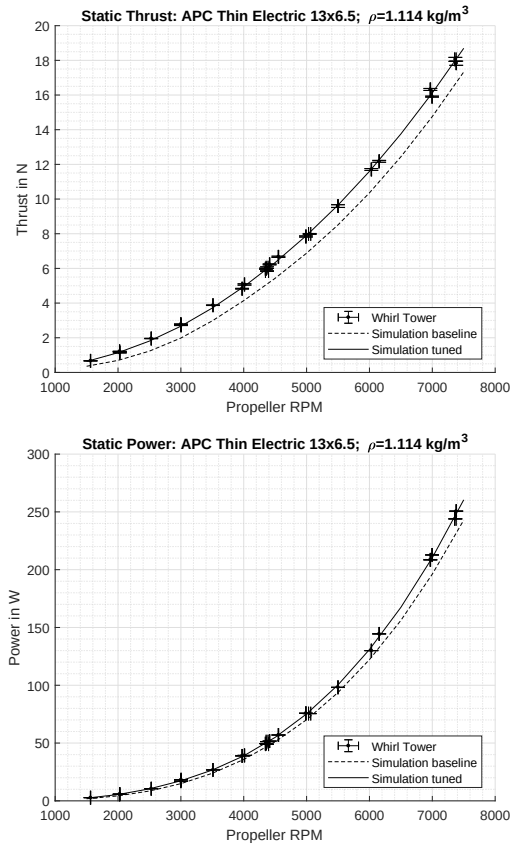

Figure 5: Static measurements for APC propeller in comparison to the initial and the tuned BE simulation.

6 Results for Propellers at an Angle of Attack

Table 1 shows the angles of attack and inflow speeds of all measurements taken. The inflow speeds were adjusted to cover the steady flight operation of a multicopter.

α_{prop} in °	8	15	22.5	30
V_∞ in m/s	8;11	8;11;15	12;15;20	17;20;30

Table 1: Range of the investigated operating conditions.

6.1 *Propeller Performance at ANDroMeDA's Design Operating Point*

At $\alpha_{prop} = 8°$ and $\alpha_{prop} = 15°$ measurements as well as simulations demonstrate, that a slightly higher thrust can be achieved with nearly the same or only a little more power. This can be seen in Figure 7. This fact is very satisfying since

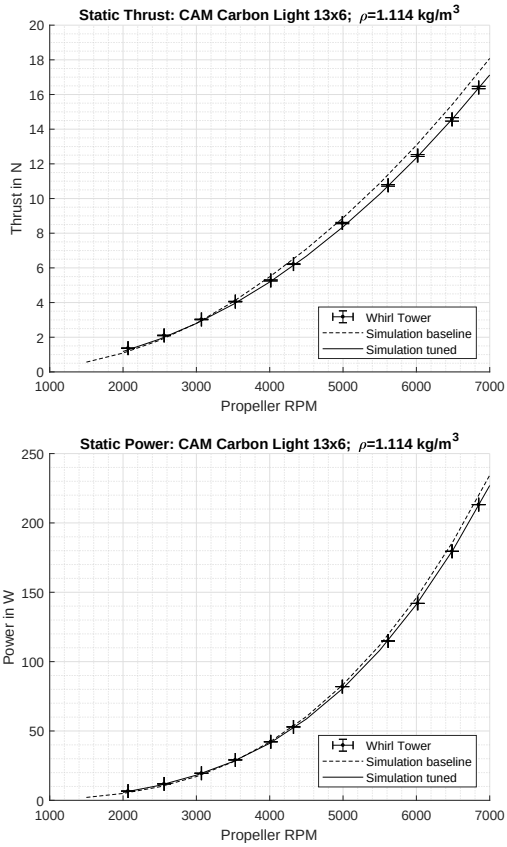

Figure 6: Static measurements for Aeronaut propeller in comparison to the initial and the tuned BE simulation.

this range of propeller angles of attack corresponds with ANDroMeDAs design operating point. Even with simple momentum theory the additional gain in thrust at the same power can be observed. Equation 1 can be used to calculate the induced velocity for an inclined propeller and hence the induced power needed for a certain thrust T:

$$P_{ind} = T \cdot (V_\infty \cdot sin(\alpha_{prop}) + v_i) \tag{7}$$

Using equation 1 and equation 7 the induced power for $\alpha_{prop} = 15°$ and $\alpha_{prop} = 30°$ at different inflow speeds can be calculated. A reduction in power can be seen for the lower angles of attack while at higher angles of attack the induced power will always be higher than in static operation (Figure 8). It has to be taken into consideration that for very low angles of attack ($\alpha_{prop} < 10°$) the reduction of induced power will be greatly overestimated by Equation 1.

6.2 *Agreement of Simulations with Measurements*

In general the *RotoCalc* simulations agree very well with wind tunnel measurements. Figure 9 depicts the worst fit at $\alpha_{prop} = 8°$ and the best fit at $\alpha_{prop} = 30°$ in case of the APC propeller. The worst agreement is a deviation from simulated

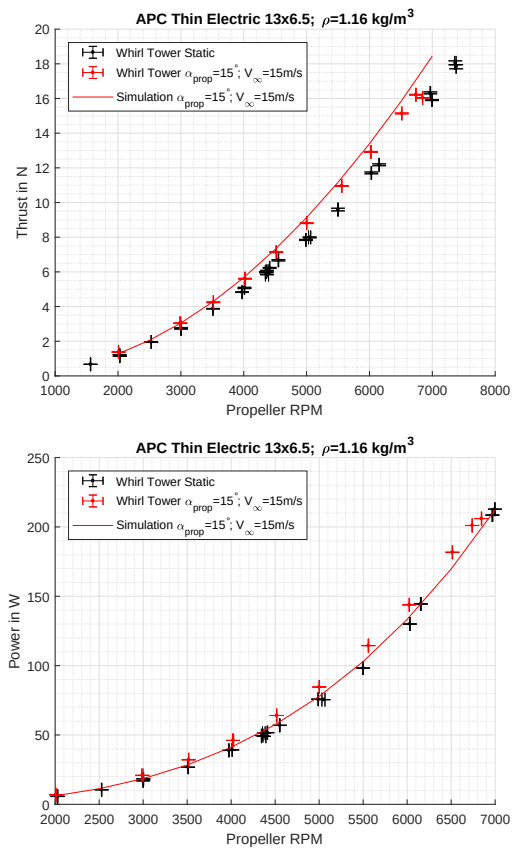

Figure 7: Thrust and power at $\alpha_{prop} = 15°$ compared to static operation.

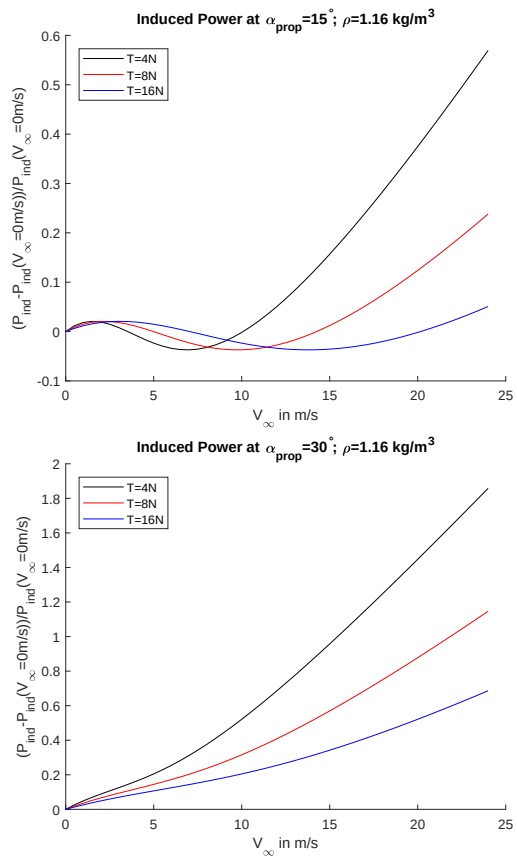

Figure 8: Induced power according to Equation 1 at different angles of attack.

power of 9.7 % and 11, 4 % from simulated thrust at $\alpha_{prop} = 8°$ at $V_\infty = 11m/s$. In most operating points the difference between measurements and simulation is much smaller.

7 Analytical Model for Inclined Propellers

A less computational and less coding intensive approach to model the performance of inclined propellers is given in [8]:

$$C_T = 0.5 \cdot cl_a \cdot \sigma \cdot (\theta_{075}/3 + 0.5 \cdot \theta_{075} \cdot \mu^2 - \lambda/2) \quad (8)$$

$$C_P = C_T^2 \cdot \kappa/(2\mu) + cd0 \cdot \sigma/8 \cdot (1 + 4.6 \cdot \mu^2) \quad (9)$$

Where $\mu = V_\infty \cdot cos(\alpha_{prop})/(\Omega r)$ is the advance ratio and $\lambda = (V_\infty \cdot sin(\alpha_{prop}) + v_i)/(\Omega r)$ is the inflow ratio. cl_a is the slope of the blade's airfoil lift polar and σ is the solidity of the rotor / propeller. θ_{075} is the blade's pitch at $r = 0.75 \cdot R$ and $cd0$ is the airfoil's zero lift drag. κ is an empirical factor accounting for tip-losses, losses of non-uniform inflow and other losses. Instead of thrust and power the dimensionless coefficients $C_T = T/(\rho \cdot A \cdot (\Omega R)^2)$ and $C_P = P/(\rho \cdot A \cdot (\Omega R)^3)$ are used.
Since the induced velocity v_i depends on the thrust from equation 1 the above expression cannot be solved analytically and the problem has to be solved numerically in an iterative manner.
This simple approach leads to a reasonable agreement of thrust at low angles of attack when the difference to the static case is low. For higher angles of attack the agreement is unfortunately of poor quality and the thrust will be significantly underestimated (Figure 10). The power was in general underestimated by this method for the investigated cases.

8 Some Observations on Counter-Rotating Propeller Configurations

In the static case the maximum thrust of the upper propeller was not influenced significantly by the operation of the lower propeller. While the thrust changed by less than 2% the power at full throttle was increased by 6%.The bottom propeller on the other hand was severely influenced by the operation of the top propeller. Maximum thrust of the bottom propeller was decreased by 30% and the power of the lower propeller was decreased by 10%.
Some theoretical background on static counter-rotating propeller operation can be found in [13]. A very simple approach

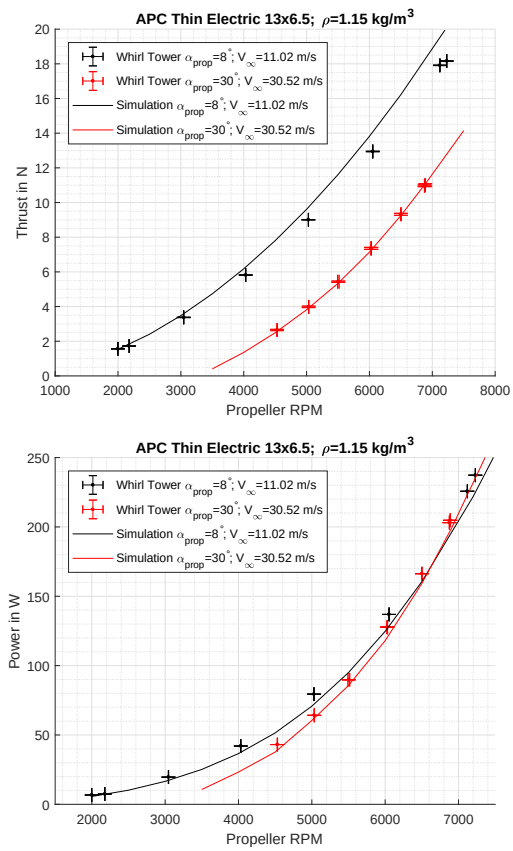

Figure 9: Agreement between measurements and simulations compared at $\alpha_{prop} = 8°$ and $\alpha_{prop} = 30°$.

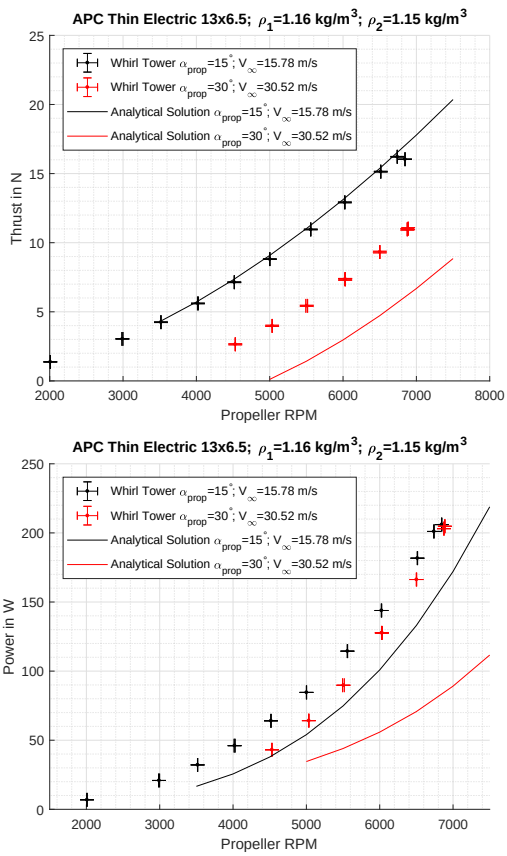

Figure 10: Analytical solution computed with Equation 8 and Equation 9.

of simulating the counter-rotating configuration is the simulation of the upper propeller as an isolated propeller and the simulation of the bottom propeller with a uniform inflow between v_i and $2v_i$ of the upper propeller. The highest uncertainty of this method is the estimation of the upper propellers wake decay. Some investigations on the wake of propellers from the authors can be found in [14].

The most interesting question that arises during the development of ANDroMeDA is how the influence of the top propeller on the bottom propeller changes when the unit is operated at higher angles of attack and higher inflow speeds. Due to strong vibrations at the test rig at forward flight conditions the full throttle test could not be repeated in the wind tunnel and another test methodology was applied: The bottom propeller was kept at a nominal thrust of about $T_{bottom} = 650\ g$ while the top propeller's thrust was slowly increased up to $T_{top} = 1000\ g$. This test gave some first insight views on the behavior in forward flight conditions compared to the static test case scenario. Table 2 compares the static test case to the forward flight case. It can be seen that in the forward flight case the bottom propeller suffers much less from the presence of the top propeller.

It is assumed that this fact is originated in the "cleaner" inflow condition for the bottom propeller in the forward flight case (Figure 11). Of course this hypothesis has to be confirmed by further measurements.

9 Conclusion and Outlook

It could be proven that static propeller measurements alone combined with blade element simulations can be sufficient to calculate the performance of a propeller in forward flight conditions as they occur at a fast flying multicopter. The error in the investigated operating conditions was always less than 10% and in the most cases a lot smaller. It has been observed that at the design operating point of the planned vehicle, ANDroMeDA even a slightly higher thrust can be achieved at nearly the same power than at static propeller operation. This could also be explained by simple momentum theory. As expected the thrust decreased greatly at higher angles of attack and higher speeds.

Another, simpler approach to model the performance of inclined propellers with less computational cost and a lot less programming effort proved to be only sufficient to predict the thrust at moderate angles of attack. At higher angles of at-

IMAV2017-44
https://www.imavs.org/pdf/imav.2017.44

	ESC Signal	Motor Current	RPM
Static Case	+9 %	+75 %	+25 %
$\alpha_{prop} = 15°$; $V_\infty = 11.88 m/s$	+4 %	+20 %	+6 %

Table 2: Changes necessary to keep the thrust of the bottom propeller steady at $T_{bottom} = 650\ g$ with the top propeller running at $T_{top} = 1000\ g$.

tack the thrust was underpredicted while the power with was always underpredicted this method. For future projects this semi-analytical approach could be adjusted to simulation or measurement data. But it seems unlikely that it is possible to model the propeller performance of arbitrary multicopter propellers at fast forwards speeds by this method without BE simulations or measurements.
Tests with a counter-rotating propeller arrangement revealed a positive effect of the propellers angle of attack and inflow speed on the operation of the bottom propeller. While the bottom propeller is influenced strongly by the wake of the top propeller this deficiency decreases at an inclined operation with some inflow speed. Unfortunately the test rig for counter-rotating propellers suffered from severe vibration so that only a few clean measurements could be taken. The proposed hypothesis has to be confirmed by further measurements in the future.

10 Acknowledgements

The ANWIND project was founded by the German Federal Ministry for Economic Affairs and Energy (BMWi). This support is gratefully acknowledged. The authors also would like to thank the Institute of Aerodynamics and Gas Dynamics at the University of Stuttgart making the wind tunnel tests possible. We would like to thank in particular Mr. Bernd Peters for his great support and advice.

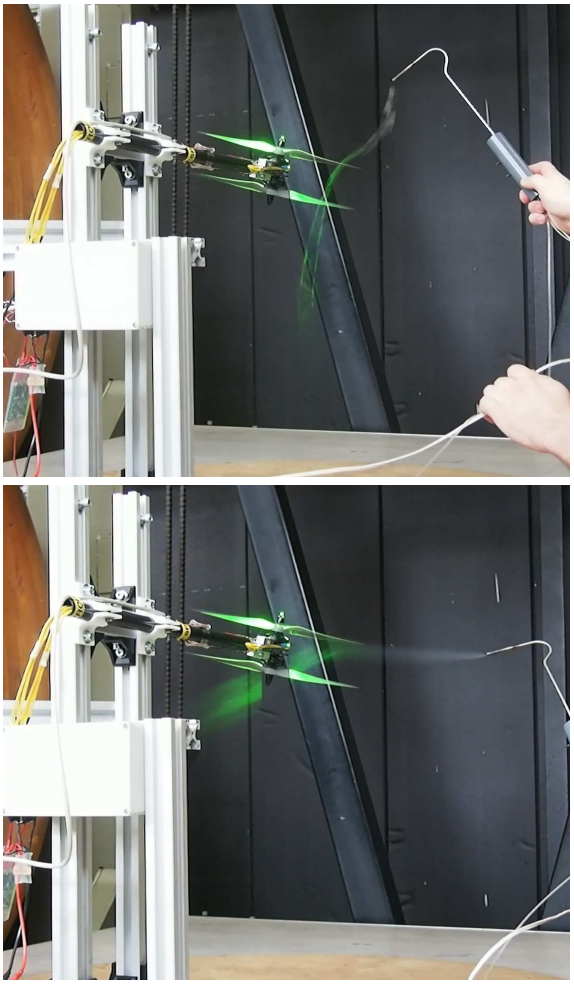

Figure 11: Smoke visualization of the counter-rotating propeller arrangement at $T = 12.5N$. Top: Static operation with wind tunnel turned off. Bottom: $\alpha_{prop} = 15°$ and $V_\infty = 11m/s$.

References

[1] M. Drela. Qprop formulation. *MIT Aero & Astro*, 2006.

[2] M. Hepperle. Javaprop user manual, 2008.

[3] M. Silvestre, J. Morgado, and J. Pascoa. Jblade: a propeller design and analysis code. In *2013 International Powered Lift Conference - AIAA AVIATION Forum*, 2013.

[4] M. Selig and J. Brandt. Propeller performance data at low reynolds numbers. *49th AIAA Aerospace Sciences Meeting AIAA 2011-1255*, 2011.

[5] W. Johnson. *A comprehensive analytical Model of Rotorcraft Aerodynamics and Dynamics*. Johnson Aeronautics, Palo Alto, California, 1988.

[6] Phidgets. Micro load cell (0-20kg) - czl635, 2016.

[7] AVIA Semiconductors. *24-Bit Analog-to-Digital Converter(ADC) for Weigh Scales*, 1 2015.

[8] W. Johnson. *Helicopter Theory*. Dover Publications, New York, NY, 2000.

[9] J. G. Leishman. *Principles of Helicopter Aerodynamics*. Cambridge University Press, Cambridge, 2002.

[10] H. Glauert. *A general Theory of the Autogyro*. Presented by the Director of scientific Research Air Ministry, Reports and Memoranda No. 111, 1926.

[11] M. Drela and H. Youngren. Xfoil 6.9 user primer. *MIT Aero & Astro*, 2001.

[12] F. Bohorquez, F. Rankinsy, J.D. Baederz, and D.J. Pinesx. Hover performance of rotor blades at low

IMAV2017-44
https://www.imavs.org/pdf/imav.2017.44

reynolds numbers for rotary wing micro air vehicles. an experimental and cfd study. In *21st Applied Aerodynamics Conference*, 2003.

[13] J. G. Leishman and A. Shreyas. An optimum coaxial rotor system for axial flight. *Journal of the American Helicopter Society*, 53(4):366–381, 2008.

[14] C. Molter and P.W. Cheng. to appear: Optimal placement of an airflow probe at a multirotor uav for airborne wind measurements. In *Proceedings of the 43rd European Rotorcraft Forum*, 2017.